

Selective excitation and structure in the continuum

C. E. Carroll* and F. T. Hioe

Department of Physics, St. John Fisher College, Rochester, New York 14618

(Received 5 August 1996)

We show that efficient transfer of molecules or atoms from one bound state to another is possible via the continuum in some cases, using two overlapping laser pulses. The structure of the continuum determines the pulse delay, laser frequencies, and laser intensities that should be used. We present simple formulas that relate the optimum values of pulse intensities, pulse separation, and detuning; these estimates can be used as a guide. More detailed calculations give quantitative results for two specific potentials. [S1050-2947(96)06412-8]

PACS number(s): 42.50.Hz, 33.80.Rv, 32.80.Rm

The concept of adiabatic population transfer from one bound state of a molecule or atom to another in a Raman-type transition via an intermediate bound state with use of two laser pulses arranged in the counterintuitive order [1] has led to numerous experimental successes [2] that are still continuing. We have suggested that the intermediate bound state can be replaced by states in the continuum [3], but our calculation was simplified by use of a flat and featureless continuum. Nakajima *et al.* [4] have pointed out that the structure of the continuum should be considered; it reduces the maximum population transfer to 61% in their calculations for one particular example. Also, they point out that unwanted laser-driven transitions to distant parts of the continuum can reduce the population transfer by a few orders of magnitude. These problems must be addressed before this technique can become a useful experimental tool. Conversely, experiments on transfer of population via the continuum may be used to infer the continuum structure.

In another approach to selective excitation, an autoionizing state is used in place of the intermediate bound state. If this state has a rather long or short lifetime, the selective-excitation process is nearly the same as with three bound states, or nearly the same as transfer through a flat continuum. This use of an autoionizing state has recently been treated by Nakajima and Lambropoulos [5]. In our calculations, no autoionizing state is explicitly recognized. We assume that no pronounced structure is found in the continuum, and treat the problem of a smooth continuum. The parameters that describe the continuum are derived from the

model of one electron moving in a potential; this is a feature of this paper. We adjust parameters of the laser pulse pair to give maximum transfer probability. This maximum is over 95% in one example. These calculations are supplemented by simple approximate formulas for the optimum laser detuning and pulse separation.

Let the two bound states have unperturbed (negative) energies E_0 and E_2 . Direct transitions between these two states are forbidden or negligible. Transitions between them and the continuum are driven by two laser beams, with carrier frequencies ω_0 and ω_2 . The intermediate states used in this stimulated Raman process occupy a narrow region of the continuum; their energies are near E and E' (Fig. 1), which satisfy $\omega_0 = (E + |E_0|)/\hbar$ and $\omega_2 = (E' + |E_2|)/\hbar$. Transitions from either bound state to the continuum occur at a rate proportional to the laser intensity. When both laser beams are present, cross terms that are proportional to the geometric-mean intensity appear. Moreover, distant parts of the continuum give rise to an ac Stark shift of each bound state relative to the bottom of the continuum and a related cross term which is emphasized by Knight, Lauder, and Dalton [6]. They show that adiabatic elimination of all continuum states can be justified if the "width" of the continuum times the laser pulse duration is large compared to \hbar . This calculation gives coupled differential equations for A_0 and A_2 , the probability amplitudes for the two bound states. Using Fermi's second golden rule to estimate the rate of unwanted laser-driven transitions to distant parts of the continuum (near F and F' in Fig. 1), we have

$$\frac{d}{dt} \begin{pmatrix} A_0 \\ A_2 \end{pmatrix} = \begin{pmatrix} -\frac{iD}{2} - (1 - iq_0)L_0(t) - s_0L_2(t) & (1 - iq_{02})\sqrt{L_0(t)L_2(t)} \\ -(1 - iq_{02})\sqrt{L_0(t)L_2(t)} & \frac{iD}{2} - (1 - iq_2)L_2(t) - s_2L_0(t) \end{pmatrix} \begin{pmatrix} A_0 \\ A_2 \end{pmatrix}, \quad (1)$$

*Also at Department of Physics and Astronomy, University of Rochester, Rochester, NY 14627.

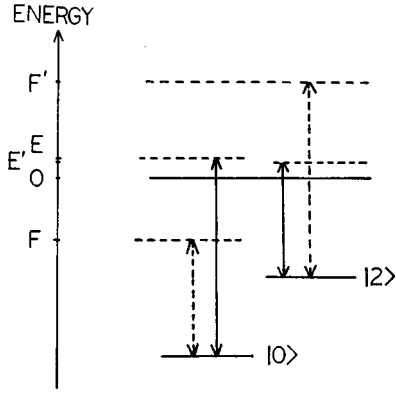


FIG. 1. Two bound states are labeled 0 and 2; continuum states are found at every positive energy. Four laser-driven transitions, including two unwanted transitions (dotted lines with double arrows) are shown.

where $L_n(t)$ is proportional to the intensity of the n th laser beam times the square of the dipole matrix element for transitions between the n th state and the continuum. Also, $D = (E - E')/\hbar$ is the mismatch of the laser frequency difference from the difference of binding energies; it is small compared to the other energies here, in order to justify the adiabatic elimination of continuum states. The continuum structure determines the dimensionless parameters q_0 , q_2 , q_{02} , s_0 , and s_2 . The first three of these depend on principal values of integrals over all energies in the continuum [6], and the ac Stark shifts are proportional to q_0 and q_2 . However, the counter-rotating term in the ac Stark shift [7] is an important correction, which is included in our computations of q_0 and q_2 ; it depends on another integral over all energies in the continuum. The dimensionless strengths of unwanted laser-driven transitions are

$$s_0 = |\langle F|x|0\rangle|^2 / |\langle E'|x|2\rangle|^2 \quad \text{and} \quad s_2 = |\langle F'|x|2\rangle|^2 / |\langle E|x|0\rangle|^2. \quad (2)$$

All five of these continuum parameters are computed, using methods described in the Appendix. After this, we find numerical solutions of Eq. (1), using the initial condition that $|A_0|^2 = 1$ and $A_2 = 0$ at the initial time.

Continuum-continuum transitions, which have been neglected in the derivation of Eq. (1), cause a rather fast apportionment of excited electrons among continuum regions that are separated by the photon energy [8]. If the laser intensity is small compared to a certain saturation intensity, we can neglect this (above-threshold ionization) effect. The

square-well model used below gives a saturation intensity above 10^{11} Watt/cm², assuming that ω_0 and ω_2 are optical frequencies. We consider intensities below 10^{11} Watt/cm², and neglect continuum-continuum transitions.

We expect selective excitation via the continuum to be feasible only when s_0 and s_2 are small. If the smaller laser frequency is too small to drive single-photon transitions from the deeply bound state to the continuum, the first of these transitions is suppressed, as in Fig. 1. Indeed, $s_0 = 0$ if F is below the continuum threshold (zero energy) and F is not the energy of a bound state. The other unwanted transition is unimportant if s_2 is small or zero. Calculations for the Coulomb potential (1s-continuum-3s) and the sech² potential (numbers appear below) show that s_2 can be much less than unity if $|E_0| \gg |E_2|$, meaning that transfer to a high-lying bound state is wanted. In other cases, $s_2 = 0$ because the bound-continuum transition matrix element changes sign at a certain energy. Such a sign change is not rare. When such a sign change affects ground-state-continuum transitions, we have a Cooper minimum [9]. Rao *et al.* [10] have recently remarked that "Cooper minima are ubiquitous for atomic and molecular systems."

If $s_0 = s_2 = 0$ and $q_0 = q_2 = q_{02}$, then solution of Eq. (1) gives population transfer close to 100%, in agreement with the conclusion of [3].

A simple solution of Eq. (1) is obtained by setting $q_0 = q_2 = s_0 = s_2 = D = 0$ and omitting the delay between laser pulses. Using $L_0(t) = L_2(t) = L(t)$, we find

$$|A_2(t)|^2 = \{\sinh^2 \mathcal{L}(t) + \sin^2[q_{02}\mathcal{L}(t)]\} \exp[-2\mathcal{L}(t)],$$

where $\mathcal{L}(t) = \int_{t_i}^t L(t') dt'$, t_i being the initial time. If $|q_{02}|\mathcal{L}(t) \approx \pi/2$ and $\mathcal{L}(t)$ is small at the end of the pulse pair, nearly complete transfer is obtained. More generally, any pair of weak pulses gives nearly complete transfer if $|q_{02}|$ is large and

$$|q_{02}| \int_{t_i}^{t_f} \sqrt{L_0(t)L_2(t)} dt \approx \pi/2, \quad (3)$$

where t_f is the final time. If the pulses are not weak, theory says that counterintuitive pulse order is required for efficient transfer to state two [1].

More generally, useful insights into solutions of Eq. (1) are obtained by applying the adiabatic approximation, in which $\vec{A} \equiv \begin{pmatrix} A_0 \\ A_2 \end{pmatrix}$ follows an eigenvector of the matrix appearing in Eq. (1); the corresponding eigenvalue is used to get the time-dependent coefficient of this eigenvector. The eigenvalues of this matrix are

TABLE I. Strengths of potentials, dimensionless energies of narrow continuum regions used as intermediaries, and calculated dimensionless parameters of the continuum.

| Potential shape | Dimensionless strength of potential | Dimensionless energy of region used | s_0 | s_2 | q_0 | q_2 | q_{02} |
|-------------------|-------------------------------------|--|-------|-----------|---------|---------|-----------|
| Sq. well | $\frac{mDw^2}{2\hbar^2} = 24$ | $\frac{mEw^2}{2\hbar^2} = 2.5916$ | 0 | 0 | -27.506 | -2.7848 | -11.180 |
| sech ² | $\frac{2mDw^2}{\hbar^2} = 6.51$ | $\frac{2mEw^2}{\hbar^2} = \frac{1}{2}$ | 0 | 0.040 325 | -6.5622 | -13.726 | -0.606 51 |

$$-\frac{(1+s_2-iq_0)L_0+(1-iq_2)L_2}{2} \pm \sqrt{\left[\frac{iD+(1-s_2-iq_0)L_0-(1-iq_2)L_2}{2}\right]^2 - L_0L_2(q_{02}+i)^2} \quad (4)$$

in the special case of $s_0=0$. Both have negative real parts, which represent transfer to the continuum. Let these eigenvalues be $\lambda_1(t)$ and $\lambda_2(t)$, two continuous complex functions of t . The corresponding eigenvectors are \vec{V}_1 and \vec{V}_2 . Suppose that the real part of $\lambda_1(t)$ is less negative than that of $\lambda_2(t)$ at early times. We assume that s_0 is zero or much less than unity, and we use the counterintuitive pulse order, so that $L_0(t)/L_2(t)$ is much less than unity at early times. Then, $\vec{V}_1 \rightarrow \binom{1}{0}$ as $t \rightarrow t_i$. The real parts of $\lambda_1(t)$ and $\lambda_2(t)$, represented by curves, may cross one or more times. The dark-state eigenvalue $\lambda_d(t)$ is defined so that its real part is less negative than the real part of the other eigenvalue, or equal to it. The real part of $\lambda_d(t)$ is continuous, but the imaginary part is generally discontinuous when the real parts of $\lambda_1(t)$ and $\lambda_2(t)$ are equal. We compute $\lambda_d(t)$ by using the upper sign in Eq. (4) and the principal value of the square root. The corresponding eigenvector is \vec{V}_d . Using the initial condition for Eq. (1), we find that \vec{A} follows \vec{V}_d at early times. Our numerical evidence suggests that, for a high probability of transfer to state two, \vec{A} follows \vec{V}_d at almost all times, even though this requires a breakdown of the adiabatic approximation near any discontinuity. This following of \vec{V}_d greatly reduces the rate of transfer to the continuum, and the probability for occupation of a bound state at the final time is approximately

$$P_b \equiv \exp \int_{t_i}^{t_f} (\lambda_d + \lambda_d^*) dt, \quad (5)$$

where λ_d^* is the complex conjugate. Computations of P_b can account for the two maxima shown in Fig. 2(b) of [4], where $\lambda_d(t)$ is continuous. If $\lambda_d(t)$ is not continuous, we have to estimate the probability that \vec{A} jumps from following \vec{V}_1 to following \vec{V}_2 ; this is done below.

We can reduce population transfer to the continuum by making the real part of λ_d vanish at one time. If $s_0 = s_2 = 0$, we make the real part of λ_d vanish by setting

$$D = (q_0 - q_{02})L_0 + (q_{02} - q_2)L_2. \quad (6)$$

If s_0 and s_2 are small rather than zero, this makes the real part of λ_d small. Since L_0 and L_2 are generally time dependent, Eq. (6) suggests that a chirp of the laser-frequency difference is desirable. If the laser frequencies are fixed, the maximum values of $L_0(t)$ and $L_2(t)$ should generally be unequal, in order to satisfy Eq. (6) approximately or to make s_0L_2 or s_2L_0 small.

In order to use a realistic pulse shape, we treat two oscillating external electric fields whose amplitudes are Gaussian functions of t , with standard deviation σ . This means

$$L_0(t) = \frac{G_0}{\sigma} \exp\left[-\frac{(t+S/2)^2}{\sigma^2}\right]$$

and

$$L_2(t) = \frac{G_2}{\sigma} \exp\left[-\frac{(t-S/2)^2}{\sigma^2}\right],$$

where S is the pulse separation. For a counterintuitive pulse pair $S < 0 < \sigma$. The dimensionless parameters of this pulse pair are G_0 , G_2 , S/σ , and $D\sigma$. Formula (6) suggests that they should satisfy

$$D\sigma = \exp(-S^2/4\sigma^2)[(q_0 - q_{02})G_0 + (q_{02} - q_2)G_2], \quad (7)$$

and Eq. (3) suggests that

$$\pi^{1/2}|q_{02}|(G_0G_2)^{1/2}\exp(-S^2/4\sigma^2) \approx \pi/2 \quad (8)$$

should hold when $|q_{02}|$ is large. These two formulas are a useful guide to choice of $D\sigma$ and S/σ .

Explicit computations of the five continuum parameters have been done for two specific one-dimensional models. We use

$$H = \frac{p^2}{2m} + V(x) \quad (9)$$

to describe the unperturbed molecule or atom; here, m and p are the electronic mass and momentum. The potential wells have width w and depth \mathcal{D} . The square-well model has

$$V(x) = \begin{cases} -\mathcal{D} & \text{for } |x| < w/2 \\ 0 & \text{for } |x| > w/2, \end{cases}$$

and the sech² model has

$$V(x) = -\mathcal{D} \operatorname{sech}^2(x/w).$$

Each potential is an even function, and we do calculations for a stimulated Raman transition from the ground state to the second excited state. These two potentials deviate from realistic atomic potentials in opposite ways. For the square well, the two jumps in $V(x)$ are too sudden; and the sech² potential is too smooth. We neglect the difference between E and E' (Fig. 1), and evaluate the five continuum parameters in ways described in the Appendix. We choose E to give $s_0=0$ and $s_2=0$ or $s_2 \ll 1$. Using the values of \mathcal{D} and E specified in Table I, we find values of s_0 , s_2 , q_0 , q_2 , and q_{02} listed in Table I. For the sech² model, there are three bound states and $|E_0| \gg |E_2|$, meaning that the second excited state is just barely bound. For the square-well model, there are four bound states.

We present some results from numerical solution of Eq. (1). For each model, we consider first pulse pairs with $G_0 = G_2$ and $D=0$, meaning that $\hbar(\omega_0 - \omega_2) = |E_0| - |E_2|$ holds exactly. The maximum probability of transfer to state two is given by pulse pairs listed as examples 1 and 3 in Table II. This probability of transfer is much greater for the square-well model than for the sech² model. For either

TABLE II. Parameters for optimal Gaussian pulse pairs, and resulting final occupation probabilities for states zero and two.

| Example number | Potential shape | Final occupation probabilities | | | | | | |
|----------------|-------------------|--------------------------------|-------|------------|-----------|--------------------|-----------|-----------------|
| | | G_0 | G_2 | S/σ | $D\sigma$ | $ A_0 ^2$ | $ A_2 ^2$ | \mathcal{P}_b |
| 1 | Sq. well | 3.96 | 3.96 | -3.39 | 0 | 5×10^{-8} | 0.712 79 | 0.712 79 |
| 2 | Sq. well | 0.269 | 0.760 | -1.78 | -4.52 | 0.004 26 | 0.950 60 | 0.954 86 |
| 3 | sech ² | 0.590 | 0.590 | -0.88 | 0 | 0.158 84 | 0.073 32 | 0.232 16 |
| 4 | sech ² | 1.290 | 0.692 | -0.15 | 0.89 | 0.082 22 | 0.258 61 | 0.340 83 |

model, this probability can be greatly increased by letting $G_0 - G_2$ and D have the same sign as $q_0 - q_2$. The maximum population transfer to state two is given by pulse pairs listed as examples 2 and 4 in Table II, and Eq. (7) gives a rough approximation to the optimum value of $D\sigma$. For all four examples, the final occupation probabilities of states zero and two are listed in Table II, along with \mathcal{P}_b , the sum of these two final occupation probabilities, or the probability of staying in a bound state. Transfer to the continuum occurs with probability $1 - \mathcal{P}_b$. We notice that \mathcal{P}_b is much greater for the square-well model than for the sech² model. For the sech² model, quite a significant amount of population remains in the ground state. Table II shows that $G_0 = G_2$ and $D = 0$ are not the best choices for transfer through a real continuum with structure. Martin, Shore, and Bergmann have found that a jump from one adiabatic path to another is sometimes necessary for efficient selective excitation, in their work on several bound states [11].

Some insight into these results can be obtained by using the adiabatic approximation, but we must count the discontinuous changes in $\lambda_d(t)$ and estimate their effect. In all four examples, $|\lambda_1(t) - \lambda_2(t)|$ has a minimum at some intermediate time. We use the Landau-Zener formula [12] to estimate the probability that \vec{A} jumps from following \vec{V}_1 to following \vec{V}_2 . We use the minimum value and the curvature of $|\lambda_1(t) - \lambda_2(t)|^2$ to compute r and s , the rapidity and separation that appear in Wannier's treatment [13] of the Landau-Zener model. The jump probability is $P_{LZ} = \exp(-\pi s^2/2r)$, which is listed in Table III; the probability of following \vec{V}_1 is $1 - P_{LZ}$. We use P_{LZ} as our estimate of the probability that \vec{A} follows \vec{V}_d when $\lambda_d(t)$ changes discontinuously, and use $1 - P_{LZ}$ as our estimate of the probability that \vec{A} follows $\vec{V}_d = \vec{V}_1$ when $\lambda_d(t)$ is continuous. The strongest pulse pair used here appears as example 1, for which P_{LZ} is small and adiabatic following is a good approximation.

In examples 1 and 3, \vec{A} follows $\vec{V}_d = \vec{V}_1$ with probability $1 - P_{LZ}$; and the estimated probability of remaining in a

TABLE III. Estimates of final occupation probabilities, based on adiabatic approximation and Landau-Zener formula.

| Example number | Discontinuities in $\lambda_d(t)$ | Estimated transfer probability | | |
|----------------|-----------------------------------|--------------------------------|----------|-------|
| | | P_b | P_{LZ} | |
| 1 | 0 | 0.783 | 0.062 | 0.735 |
| 2 | 1 | 0.980 | 0.981 | 0.962 |
| 3 | 0 | 0.413 | 0.922 | 0.032 |
| 4 | 1 | 0.504 | 0.952 | 0.480 |

bound state is Eq. (5). Hence, the estimated probability of transfer to state two is $P_b(1 - P_{LZ})$. In examples 2 and 4, $\lambda_d(t)$ is a function with one jump discontinuity, which implies a jump in \vec{V}_d . Transfer to state two requires \vec{A} to follow this jump. This occurs with probability P_{LZ} , and $P_b P_{LZ}$ is the probability of transfer to state two. For all four examples, this estimated probability appears in the last column of Table III, which should be compared with the next-to-last column in Table II. The adiabatic approximation has been combined with the Landau-Zener formula, to estimate the probability of transfer to state two. This estimate is much more accurate for the square-well examples than for the sech² examples. We have used P_b , given by Eq. (5), as our estimate of \mathcal{P}_b ; this estimate is also much more accurate for the square-well examples than for the sech² examples.

All these calculations have used potentials with three and four bound states. As the Rydberg series is absent, these models have a resemblance to negative ions. Recent measurements and calculations [14] show that some negative ions have several bound states. Our results may be applicable to some negative ion, but we do not exclude application to neutral molecules and atoms.

We also report some numerical results for the symmetrical special case of $q_0 = q_2 = s_0 = s_2 = 0$, which was previously studied in [4] and [15]. The highest probability of transfer to state two is obtained by using $G_0 = G_2$ and $D = 0$. The maximum transfer probabilities are listed in Table IV, along with the values of $G = G_0 = G_2$ and $|q| = |q_{02}|$. Although the assumption that $|q| \neq 0$ reduces the probability of transfer to state two, the pulse pair can always be arranged to give more than 54% transfer. If $|q|$ is rather small or rather large, the maximum transfer probability is close to 100%. The last column of Table IV shows how $\pi^{1/2}|q|G \exp(-S^2/4\sigma^2)$ approaches $\pi/2 \approx 1.57$ as $|q|$ increases; this agrees with Eq. (8). For a fixed value of $|q|$, we find that quite a range of values of G and S/σ give transfer probabilities near the maximum, if the product

TABLE IV. Maximum probability of transfer for various values of $|q| = |q_{02}|$.

| $ q $ | G | S/σ | $ A_2 ^2$ | $\pi^{1/2} q G \exp(-S^2/4\sigma^2)$ |
|-------|-------|------------|-----------|--------------------------------------|
| 0.25 | 9.41 | -1.47 | 0.764 00 | 2.43 |
| 0.5 | 4.39 | -1.52 | 0.631 75 | 2.18 |
| 1.0 | 2.16 | -1.72 | 0.546 62 | 1.83 |
| 2.0 | 1.12 | -1.87 | 0.579 73 | 1.66 |
| 4.0 | 0.564 | -1.92 | 0.690 83 | 1.59 |
| 8.0 | 0.290 | -1.96 | 0.806 35 | 1.57 |

$G \exp(-S^2/4\sigma^2)$ is kept nearly constant; see [15]. In the case of $|q|=4$, the transfer probability varies from 0.654 42 to 0.690 83 to 0.623 65 and $G \exp(-S^2/4\sigma^2)$ varies from 0.199 to 0.316 when G varies from 0.25 to 64.

Some physical effects not represented in Eq. (1) should be mentioned. In a more elaborate treatment of two bound states and a continuum, the ac Stark shifts of state zero by laser beam two and state two by laser beam zero would be taken into account; this would turn s_0 and s_2 into complex coefficients. Also, further counter-rotating terms would be taken into account. We believe that treatment of these additional terms would not greatly affect the results of our calculations.

We conclude that the effects of continuum structure and unwanted laser-driven transitions can be overcome, by appropriate choices of pulse separation, laser frequencies, and laser intensities. This means that population transfer through the continuum can be realized. The best laser intensities for this process are generally quite moderate, unlike those in the original calculation [3]. Although the process cannot always be regarded as adiabatic transfer, relations (7) and (8) may give a useful guide to optimum pulse parameters. Also, these relations can be used to interpret experimental data in terms of continuum structure.

Note added in proof. We have received a manuscript by Yatsenko, Unanyan, Bergmann, Halfmann, and Shore that describes similar calculations.

ACKNOWLEDGMENTS

We want to thank Eric Shaner for help with some computations. This research was supported by NSF Grant PHY-9507837.

APPENDIX

Five dimensionless parameters that describe the continuum appear in Eq. (1), and we compute them for a model

described by Eq. (9). It is not difficult to find eigenfunctions of Eq. (9) for the potentials $V(x)$ used here. We mention that associated Legendre functions [16] are used for the sech^2 shape. Their degree is ν ($=2.1$ for the case listed in Table I), and $2mDw^2/\hbar^2 = \nu(\nu+1)$. Their order is μ , which is imaginary for the continuum wave functions. When eigenfunctions of Eq. (9) are known, evaluation of Eq. (2) is straightforward. However, q_0 , q_2 , and q_{02} involve sums over all odd eigenfunctions, as we treat transfer from one even bound state to another. Each sum includes a sum over odd bound states and an integration over odd continuum states. We have five of these sums, because counter-rotating terms in q_0 and q_2 are computed. For the square-well potential, these five sums over odd eigenfunctions are easily evaluated by using two functions of z

$$\left\langle eb \left| x \frac{1}{z-H} x \right| eb \right\rangle \quad \text{and} \quad \left\langle eb \left| x \frac{1}{z-H} x \right| eb' \right\rangle.$$

Here, z is the complex variable and the kets $|eb\rangle$ and $|eb'\rangle$ describe two different even bound states. Although these are elementary functions of z , the explicit formulas are too long to quote here. These formulas are evaluated at $z = E + i0^+$, in order to evaluate the principal-value integrals indirectly. The counter-rotating term in q_n is obtained from

$$\left\langle eb \left| x \frac{1}{E - 2\hbar\omega_n - H} x \right| eb \right\rangle.$$

This calculation of q_0 , q_2 , and q_{02} for the square-well model is entirely analytic, apart from preliminary solution of a transcendental equation for

$$\frac{m|E_0|w^2}{2\hbar^2} \quad \text{and} \quad \frac{m|E_2|w^2}{2\hbar^2},$$

the two-dimensionless binding energies.

-
- [1] F. T. Hioe, Phys. Lett. A **99**, 150 (1983); J. Oreg, F. T. Hioe, and J. H. Eberly, Phys. Rev. A **29**, 690 (1984); C. E. Carroll and F. T. Hioe, J. Opt. Soc. Am. B **5**, 1335 (1988); Phys. Rev. A **42**, 1522 (1990); J. R. Kuklinski, U. Gaubatz, F. T. Hioe, and K. Bergmann, *ibid.* **40**, 6741 (1989); Y. B. Band and P. S. Julienne, J. Chem. Phys. **94**, 5291 (1991); P. Marte, P. Zoller, and J. L. Hall, Phys. Rev. A **44**, 4118 (1991).
- [2] U. Gaubatz, P. Rudecki, S. Schieman, and K. Bergmann, J. Chem. Phys. **92**, 5363 (1990); S. Schieman, A. Kuhn, S. Steuerwald, and K. Bergmann, Phys. Rev. Lett. **71**, 3637 (1993); J. Lawall and M. Prentiss, *ibid.* **72**, 993 (1994); L. S. Goldner *et al.*, *ibid.* **72**, 997 (1994); A. Kasapi, M. Jain, G. Y. Yin, and S. E. Harris, *ibid.* **74**, 2447 (1995); J. Martin, B. W. Shore, and K. Bergmann, Phys. Rev. A **54**, 1556 (1996).
- [3] C. E. Carroll and F. T. Hioe, Phys. Rev. Lett. **68**, 3523 (1992); Phys. Lett. A **199**, 145 (1995).
- [4] T. Nakajima, M. Elk, J. Zhang, and P. Lambropoulos, Phys. Rev. A **50**, 913 (1994).
- [5] T. Nakajima and P. Lambropoulos, Z. Phys. D **36**, 17 (1996).
- [6] P. L. Knight, M. A. Lauder, and B. J. Dalton, Phys. Rep. **190**, 1 (1990).
- [7] I. I. Sobelman, *Atomic Spectra and Radiative Transitions*, 2nd ed. (Springer-Verlag, Berlin, 1992), Chap. 7.
- [8] Z. Deng and J. H. Eberly, Phys. Rev. Lett. **53**, 1810 (1984).
- [9] J. W. Cooper, Phys. Rev. **128**, 681 (1962); T. A. Carlson *et al.*, Z. Phys. D **2**, 309 (1986).
- [10] R. M. Rao, E. D. Poliakoff, K. Wang, and V. McKoy, Phys. Rev. Lett. **76**, 2666 (1996).
- [11] J. Martin, B. W. Shore, and K. Bergmann, Phys. Rev. A **52**, 583 (1995).
- [12] L. Landau, Phys. Z. Sowjetunion **2**, 46 (1932); C. Zener, Proc. R. Soc. London Ser. A **137**, 696 (1932).
- [13] G. H. Wannier, Physics (N.Y.) **1**, 251 (1965).
- [14] J. Thøgersen, M. Scheer, L. D. Steele, H. K. Haugen, and W. P. Wijesundera, Phys. Rev. Lett. **76**, 2870 (1996); Z. Liu and P. B. Davies, *ibid.* **76**, 596 (1996); K. Dinov, D. R. Beck, and D. Datta, Phys. Rev. A **50**, 1144 (1994).
- [15] C. E. Carroll and F. T. Hioe, in *Coherence and Quantum Optics VII*, Proceedings of the Rochester Conference, edited by J. H. Eberly, L. Mandel, and E. Wolf (Plenum, New York, 1996), p. 527.
- [16] A. Erdélyi, W. Magnus, F. Oberhettinger, and F. G. Tricomi, *Higher Transcendental Functions* (McGraw-Hill, New York, 1953), Vol. 1, Chap. 3.